



HAL
open science

Accurate Potential Energy Curves for $Tl+-Rg$ ($Rg = He-Rn$): Spectroscopy and Transport Coefficients

Timothy Wright

► **To cite this version:**

Timothy Wright. Accurate Potential Energy Curves for $Tl+-Rg$ ($Rg = He-Rn$): Spectroscopy and Transport Coefficients. *Molecular Physics*, 2007, 104 (20-21), pp.3237-3244. 10.1080/00268970601075246 . hal-00513058

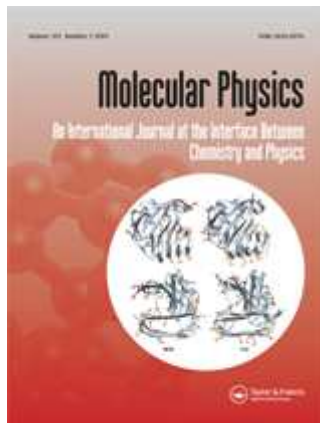
HAL Id: hal-00513058

<https://hal.science/hal-00513058>

Submitted on 1 Sep 2010

HAL is a multi-disciplinary open access archive for the deposit and dissemination of scientific research documents, whether they are published or not. The documents may come from teaching and research institutions in France or abroad, or from public or private research centers.

L'archive ouverte pluridisciplinaire **HAL**, est destinée au dépôt et à la diffusion de documents scientifiques de niveau recherche, publiés ou non, émanant des établissements d'enseignement et de recherche français ou étrangers, des laboratoires publics ou privés.



**Accurate Potential Energy Curves for Tl^+-Rg ($Rg = He-Rn$):
Spectroscopy and Transport Coefficients**

Journal:	<i>Molecular Physics</i>
Manuscript ID:	TMPH-2006-0005.R1
Manuscript Type:	Full Paper
Date Submitted by the Author:	10-Oct-2006
Complete List of Authors:	Wright, Timothy; University of Nottingham, School of Chemistry
Keywords:	potential energy curves, transport coefficients, spectroscopy, complexes



Accurate Potential Energy Curves for $Tl^+ - Rg$ ($Rg = He - Rn$): Spectroscopy and Transport Coefficients

Benjamin R. Gray^a, Edmond P. F. Lee^b, Ahlam Yousef^c, Shraddha Shrestha^c,
Larry A. Viehland^{c 1}, and Timothy G. Wright^{a 2}

^a School of Chemistry, University of Nottingham, University Park, Nottingham, NG7
2RD, UK

^b School of Chemistry, University of Southampton, Highfield, Southampton, SO17
1BJ, UK and Department of Applied Biology and Chemical Technology, Hong Kong
Polytechnic University, Hung Hom, Hong Kong.

^c Division of Science, Chatham College, Pittsburgh, PA 15232, USA

¹ email: viehland@chatham.edu

² email: Tim.Wright@nottingham.ac.uk

Abstract

High-quality *ab initio* potential energy curves are presented for the $Tl^+ - Rg$ series ($Rg = He - Rn$). Calculations are performed at the CCSD(T) level of theory, employing aug-cc-pV5Z quality basis sets, with “small core” relativistic effective core potentials being used for Tl^+ and $Kr - Rn$. The curves are shown to be in excellent agreement with experimental mobility data for the systems $Tl^+ - Rg$ ($Rg = He - Xe$), and generally excellent agreement is also obtained with longitudinal diffusion data. An exception to the latter is Tl^+ in He, which is attributed to the experimental data not being obtained under steady state conditions. We also present spectroscopic information for the titular species, derived from our potential energy curves, and compare the results to previous potentials inferred from the ion transport data.

1. Introduction

This work continues our series of studies focused on the production of accurate atomic ion/rare gas atom interaction potentials. In this paper, as with the others in the series, we employ the potentials to obtain transport coefficients and spectroscopic data and compare these to experiment and theory where data are available. Other papers in this series concern: the 36 alkali metal/Rg systems;^{1, 2, 3, 4} O⁻ with He, Ne and Ar;⁵ S⁻ with He;⁶ Hg⁺ and Cd⁺ with all six Rg;⁷ O⁺ with He;⁸ F⁻ with all of the Rg;⁹ and Br⁻ with all of the Rg.¹⁰ One of us has also looked at ³He⁺ and ⁴He⁺ in their parent gases,¹¹ the Cl/Rg systems¹² and the I/Rg systems.¹³ In this paper we present six new interaction potentials between the group 13 ion, Tl⁺, and the rare gas atoms, Rg. The only previously-reported potentials appear to be the “directly determined” (DD) potentials¹⁴, i.e. those obtained from measurements^{15, 16, 17, 18, 19} of the gas-phase ion transport properties by inversion^{20, 21}. (Note that the smoothed versions of the original data^{15, 16, 17} used herein are reported in refs. 18, 19.)

The purpose of the present work is to determine *ab initio* potential energy curves for the Tl⁺-Rg systems over wide ranges of the ion-neutral separations. The potentials are employed to calculate spectroscopic constants and gaseous ion transport data. Where available, we compare these to the experimental and theoretical results mentioned above.

2. Computational Details

The potential energy curves were calculated point by point at the restricted coupled cluster level²², RCCSD(T), with single and double excitations and with the non-iterative correction to triple excitations, using the MOLPRO²³ suite of programs. The full counterpoise (CP) correction was employed at each point to correct for basis set superposition error (BSSE).

The calculations were run with augmented, all-electron quintuple- ζ basis sets (aug-cc-pV5Z) for He, Ne and Ar. We employed the “small-core” effective core potentials ECP10MDF, ECP28MDF and ECP60MDF for Kr, Xe and Rn, respectively; and an ECP60MDF one for Tl⁺. Tl has the electronic configuration, $\dots 5s^2 5p^6 5d^{10} 6s^2 6p^1$, and so the ground state is a ¹S state, with $\dots 6s^1 6p^1$ states lying $\sim 50,000$ cm higher in energy²⁴, and so not expected to interact with the ground state. There is a complication present in running these calculations, since the ordering of the orbitals changes. The Tl⁺ 5s and 5p orbitals lie above the 1s2s2p orbitals of Ar, and the 1s orbitals of Ne and He, and are correlated; but for the heavier rare gas atoms, the Tl⁺ 5s and 5p orbitals are lower

1
2 than the valence electrons, and are uncorrelated. This places different demands on the thallium
3 basis set, and tight basis functions need to be added in to describe better the correlation of the “outer
4 core” $5s5p$ electrons. Thus, for the $Tl^+ - Rg$ complexes involving the lighter three rare gas atoms,
5 the thallium basis set was as follows: the ECP60MDF ECP was employed, with the standard aug-
6 cc-pV5Z valence basis set, further augmented by tight functions: three s functions ($\zeta = 10.0, 4.0$ and
7 1.6); three sets of p functions ($\zeta = 9.375, 3.75$ and 1.5); two d functions ($\zeta = 3.125$ and 1.25); two f
8 functions ($\zeta = 3.125$ and 1.25); a set of g functions ($\zeta = 1.35$); and a set of h functions ($\zeta = 1.35$).
9 For the calculations on $Tl^+ - Rg$ complexes involving the three heavier rare gas atoms, the additional
10 s and p functions were omitted, as were the additional tightest set of d and f functions. All standard
11 exponents and contractions were taken from the MOLPRO internal library. Once the counterpoise-
12 corrected energy points were obtained, they were used as input to LeRoy’s LEVEL²⁵ program, from
13 which we were able to calculate equilibrium nuclear separations, dissociation energies, and
14 rovibrational energy levels.
15
16
17
18
19
20
21
22
23
24
25
26
27

28 Transport cross-sections and coefficients were calculated from the interaction potentials as a
29 function of ion-neutral collision energy using the programs QVALUES and GRAMCHAR.^{26,27,28}
30 The accuracies of the calculated mobilities and diffusion coefficients were 0.1% and 1.0%,
31 respectively, unless otherwise noted below.
32
33
34
35
36
37

38 3. Results

39 A. Potential Curves

40 The six potential curves are plotted in Figure 1 and the tabulated values (which extend both to
41 smaller and larger separation) are available from the authors upon request. The only other potential
42 energy curves available, the directly-determined ones, are shown in Figure 2, plotted against the
43 present curves. The differences between the present and the previous results will be discussed
44 briefly in this section, and in more detail after their abilities to reproduce the transport data are
45 discussed in the next section.
46
47
48
49
50
51
52
53
54
55

56 The parameters for each of our calculated potentials are given in Table I. They are: the separation,
57 σ , at which the interaction energy is zero (on the repulsive wall); the equilibrium separation, R_e , at
58 which the potential energy reaches its minimum value; and D_e , which is the depth of the potential
59 well. The parameters show monotonic trends down the Rg group, with smooth decreases in σ and
60 R_e and a reasonably smooth decrease in D_e —the non-periodicity of the directly-determined

parameters¹⁴ was attributed to errors in the original transport data.

For $\text{TI}^+\text{-He}$, the DD potential encompasses only a fragment of the repulsive wall and the start of the potential well. The DD wall is steeper and the zero energy separation is 0.25 \AA shorter than our potential, suggesting that the complete potential would probably be too strongly bound. For $\text{TI}^+\text{-Ne}$, part of the repulsive wall is given by the DD potential as well as the potential well. Again, the wall is steeper and the zero energy value is 0.27 \AA shorter than our potential. Here we can also compare the equilibrium separation and the dissociation energy. The potential is too strongly bound, has too short an equilibrium separation, and has too deep a well, compared to the present potential. At around 3.2 \AA our potential and the DD potential cross (see Figure 2) and the latter appears to approach the dissociation limit above our curve.

For $\text{TI}^+\text{-Ar}$, the behaviour is similar to Ne, with shorter zero energy and equilibrium distances, a deeper well, and a steeper repulsive wall. This time, however, the difference in dissociation energy is more pronounced, with the DD potential being almost twice as deep as the present potential, and with a bond length that is 0.7 \AA shorter. The trend continues for $\text{TI}^+\text{-Kr}$ where a similarly large dissociation energy results from the DD potential, and a bond length that is 0.5 \AA too short.

For $\text{TI}^+\text{-Xe}$, only a short section of the attractive region of the potential was previously generated to which to compare. The curves appear to be converging asymptotically to large R , but again, the trend suggests that the DD potential is too attractive. The results given here for $\text{TI}^+\text{-Rn}$ appear to be the only ones available.

B. Spectroscopic Data

Our calculated spectroscopic parameters are given in Table II. The dissociation energy, D_0 , is given as computed, while the vibrational constants, ω_e and $\omega_e x_e$, have been determined from the energies of the three lowest vibrational levels with rotational quantum number $J = 0$. The rotational constant, B_0 , and the centrifugal distortion constant, D_{J0} , have been obtained by fitting the energies of the three lowest rotational energy levels for vibrational quantum number $v = 0$ to the standard energy expression.

There are no experimental results with which to compare our values.

C. Transport Data

Gaseous ion mobility and diffusion coefficients serve as good tests of the accuracy of ion-neutral interaction potentials over wide ranges of internuclear separation. This is because the data are often available with fair to high accuracies over wide ranges of the gas temperature, T_0 , and of the ratio, E/n_0 , of the electrostatic field strength to the gas number density in the drift-tube mass spectrometers used for the experiments²⁹.

We have calculated diffusion coefficients and mobilities for thallium cations in the rare gases over wide ranges of E/n_0 and at a variety of T_0 , and we have placed the results in the gaseous ion transport database at Chatham College³⁰. In Fig. 3, we show the calculated mobilities at 300 K as compared to the experimental values, with a corresponding comparison for diffusion coefficients being presented in Figure 4. Statistical comparisons²¹ at 300 K are shown in Tables III and IV, where N is the number of experimental values in the indicated range of E/n_0 , "Acc" is the estimated accuracy given by experiment and "Prec" is the precision of our numerical calculations. The statistical quantity δ is small if there is good agreement, with values above 1 or below -1 indicating that the experimental values are significantly above or below the calculated values, respectively. The statistical quantity χ is always positive and should not be much greater than $|\delta|$; larger values indicate either that the data is scattered or that the comparison is significantly dependent upon E/n_0 .

For Tl^+ in He, the mobility values in Table III indicate that the potential is performing extremely well, as the $|\delta|$ values are almost zero. However the $|\delta|$ value for the products, $n_0 D_L$, of the gas number density and the ion diffusion coefficient parallel to the electrostatic field, given in Table IV, are greater than 1, suggesting disagreement with experiment, as can be seen in Figure 4. It was noted in the original experimental paper¹⁷ that there was disagreement between the $n_0 D_L$ values predicted from the mobilities by generalized Einstein relations, despite these relations giving good agreement for Tl^+ moving in Ne and Ar. It was concluded that the Tl^+ ions had not reached a steady state in the drift tube filled with He, owing to the mass mismatch, and that this would lead to disagreement with the calculated values, as was observed.

Transport properties calculated from the DD potential for Tl^+ -He are in approximately as good agreement with the data as the present potential, even though the potentials themselves differ significantly. We attribute this to the limited range of separations (4.20-5.40 bohr) that significantly influence the transport coefficients over the small range of E/n_0 used in the experiments and the rather smooth behaviour of the potential on this region of the repulsive wall. The DD procedure

1 requires knowledge of the position of the potential minimum, and without such knowledge it can
2 lead to many different potentials that describe the experimental data with about the same accuracy.
3 We conclude that the present potential is accurate based on the good agreement of the present
4 potential with the mobility data, and the recognized weakness of the experimental diffusion values.
5 In addition, the good agreement for the other systems (*vide infra*), using the same methodology,
6 also indicates that this potential is accurate.
7
8
9
10
11
12

13
14 For TI^+ in Ne, we again observe extremely small values for $|\delta|$ values for the mobilities calculated
15 from the present potential, but this time we also obtain small values for the diffusion coefficients.
16 Thus both sets of data show excellent agreement through all regions of E/n_0 , and this may also be
17 seen in Figures 3 and 4. The good agreement with the diffusion data is in line with the good
18 agreement achieved in ref. 17 between the experimental and generalized Einstein relation values.
19 The values of $|\delta|$ are smaller than those reported in ref. 14 for the DD potential, although those
20 values are also less than 1. The experimental data for this system probes the repulsive wall and
21 only a small portion of the well, *i.e.* separations between 4.6 and 6.8 bohr, so the DD potential
22 directly inferred from these data are expected to have only fair accuracy, as shown in Fig. 2. We
23 conclude that our current potential is accurate.
24
25
26
27
28
29
30
31
32

33
34 For TI^+ in Ar, our potential is in exceptionally good agreement with the mobility results over the
35 whole range of E/n_0 — see Table III and Figure 3. For the diffusion data, the results in Table IV are
36 broken into two groups, between $E/n_0 = 10$ –150 Td ($1 \text{ Td} = 10^{-21} \text{ Vm}^2$) and $E/n_0 = 150$ –350 Td.
37 The lower E/n_0 data shows good agreement between experiment and theory, however for the larger
38 E/n_0 values, the value of $|\delta|$ suggests a significant disagreement between the calculated experimental
39 and calculated data, although the $|\delta|$ value for the whole range is still good. Figure 4 shows this as
40 well, with the calculated diffusion data just coming outside the error bars at high E/n_0 . This is
41 likely a reflection of the known inaccuracies of the Georgia Tech diffusion data at high E/n_0 , owing
42 to an inadequate treatment of the raw arrival time spectra.³¹
43
44
45
46
47
48
49
50

51
52 TI^+ in Kr continues the trend in this present series of potentials by producing excellent agreement
53 between experiment and theory over a very wide range of E/n_0 values, with good agreement seen
54 within each of the ranges as well. The indications are that the potential is consistent with the
55 experimental data over long-, mid- and short- R values — see Tables III and IV and Figures 3 and 4.
56 A very similar story holds for TI^+ in Xe, and similar conclusions are drawn. There is no
57 experimental data with which to compare TI^+ in Rn, but since the methodology is the same, we
58 assume that the potential is of a similar reliability.
59
60

4. Conclusions

We have calculated Tl^+ -Rg potentials over a wide range of separation, and have found that the potentials are in excellent agreement overall with the available experimental data, well within the 3-4% error bars on the mobility, and also generally within the 12-14% error bars on the diffusion data. The level of theory employed is high, using the RCCSD(T) correlated method and large basis sets, with small-core ECPs for the heavier atoms. We have noted that the $5s$ and $5p$ Tl^+ orbitals lie above the valence orbitals of He, Ne and Ar, but below those of Kr, Xe and Rn. We chose to correlate these for the lighter atoms, and included appropriate basis functions in the basis set to account for this.

The only poor result is that observed for Tl^+ in He with respect to the value for the product, $n_0 D_L$, of the gas number density and the ion diffusion coefficient parallel to the electrostatic field, given in Table IV. We have noted, however, that the original experimenters pointed out a disagreement between the data and an approximate theoretical model, and concluded that their experimental data was affected by the failure of the light helium to allow steady state conditions to be reached. In light of this, and the overall good agreement for the other systems, we conclude that the present calculated transport data is more reliable than the experimental data. The only other region of disagreement was with the Ar high E/n_0 data for $n_0 D_L$, and again, it is probably safe to assume that the experimental data is unreliable.

In summary, apparently for the first time, we have presented tested potential energy curves for a cation of a sixth-period element, interacting with each of the Rg atoms, and have shown that these curves are in excellent agreement with the only available experimental data, and are thus accurate descriptions of the Tl^+ -Rg interactions.

Acknowledgements

BRG is grateful for support via a studentship from the EPSRC. The authors are grateful to the EPSRC for the award of computer time at the Rutherford Appleton Laboratories under the auspices of the Computational Chemistry Working Party (CCWP), which enabled these calculations to be performed. The research of LAV was supported by the U. S. National Science Foundation under grant CHE-0414241.

Table I. Parameters derived from the present $Tl^+ - Rg$ interaction potentials, compared to those from ref. 14. (See text for details.)

Potential	Ref.	$\sigma / \text{\AA}$	$R_e / \text{\AA}$	D_e / cm^{-1}
$Tl^+ - He$	present	2.85	3.28	119.0
	KV	2.60	^a	^a
$Tl^+ - Ne$	present	2.81	3.23	263.1
	KV	2.54	2.85	372.0
$Tl^+ - Ar$	present	2.85	3.32	919.0
	KV	2.50	2.64	1600.6
$Tl^+ - Kr$	present	2.89	3.38	1295.3
	KV	2.54	2.86	2149.3
$Tl^+ - Xe$	present	2.96	3.48	1870.7
	KV	^a	^a	^a
$Tl^+ - Rn$	present	2.97	3.50	2262.0

^a Curve derived in ref. 14, but portion was not wide enough to establish this parameter.

Table II. Calculated spectroscopic constants in cm^{-1} , with numbers in parentheses denoting the power of ten. (See text for details.)

System	D_0	ω_e	$\omega_e x_e$	B_0	D_{j0}
$\text{Tl}^+\text{-He}$	119.0	63.04	8.87	0.365	6.49(-05)
$\text{Tl}^+\text{-Ne}$	263.2	49.42	2.68	0.0865	1.22(-06)
$\text{Tl}^+\text{-Ar}$	919.1	62.46	1.20	0.0454	1.01(-07)
$\text{Tl}^+\text{-Kr}$	1295.3	53.44	0.62	0.0247	2.18(-08)
$\text{Tl}^+\text{-Xe}$	1870.7	52.84	0.41	0.0174	7.68(-08)
$\text{Tl}^+\text{-Rn}$	2262.0	49.33	0.29	0.0129	3.58(-09)

Table III. Statistical Comparison of Calculated and Experimental Mobility Data at 300 K.^a

System	Expt. Data	E/n_0 Range	N	Acc	Prec	δ	χ
Tl ⁺ -He	Smooth	6.0-60.0	8	4.00	0.02	0.05	0.25
	Raw	6.0-70.0	20	4.00	0.02	0.15	0.22
Tl ⁺ -Ne	Smooth	7.0-100.0	9	4.00	0.02	-0.07	0.18
	Raw	7.0-81.4	40	4.00	0.02	0.09	0.27
Tl ⁺ -Ar	Smooth	10.0-150.0	9	4.00	0.10	0.09	0.19
		150.0-350.0	4	4.00	0.10	0.03	0.08
		10.0-350.0	13			0.07	0.16
	Raw	10.0-150.0	45	4.00	0.10	0.15	0.47
		150.0-369.0	34	4.00	0.10	0.01	0.49
		10.0-369.0	79			0.09	0.48
Tl ⁺ -Kr	Smooth	20.0-80.0	7	3.00	0.02	0.12	0.13
		80.0-700.0	11	3.00	0.10	-0.33	0.40
		20.0-700.0	18			-0.16	0.33
	Raw	20.1-80.0	17	3.00	0.02	0.14	0.33
		80.0-710.1	57	3.00	0.10	-0.27	0.59
		20.1-710.1	74			-0.18	0.54
Tl ⁺ -Xe	Smooth	25.0-120.0	8	3.00	0.10	0.21	0.22
		120.0-350.0	5	3.00	0.50	-0.01	0.16
		25.0-350.0	13			0.13	0.20
	Raw	25.1-120.0	14	3.00	0.10	0.22	0.37
		120.0-352.4	28	3.00	0.50	0.12	0.58
		25.1-352.4	42			0.16	0.52

^a Calculated mobilities were obtained from the present potential. The smooth experimental data were taken from Ref. 18 and the raw experimental data were obtained from the gaseous ion transport database in Ref. 28.

Table IV. Statistical Comparison of Calculated and Experimental Values of n_0D_L at 300 K.^a

System	Expt. Data	E/n_0 Range	N	Acc	Prec	δ	χ
Tl ⁺ -He	Smooth	6.0–35.0	9	12.0	1.00	1.31	1.66
	Raw	6.0–35.0	15	12.0	1.00	1.45	1.95
Tl ⁺ -Ne	Smooth	7.0–110.0	12	15.0	1.00	0.42	0.58
	Raw	7.0–81.4	71	15.0	1.00	0.29	0.55
Tl ⁺ -Ar	Smooth	7.0–150.0	9	12.0	1.00	0.22	0.59
		150.0–350.0	4	12.0	3.00	1.19	1.19
	Raw	7.0–350.0	13			0.52	0.83
		10.0–150.0	46	12.0	1.00	0.16	0.54
		150.0–250.0	28	12.0	2.00	0.72	0.98
		250.0–369.0	14	12.0	3.00	1.13	1.23
	10.0–369.0	88			0.49	0.84	
Tl ⁺ -Kr	Smooth	2.0–90.0	5	13.0	1.00	0.48	0.61
		90.0–800.0	11	13.0	2.00	0.02	0.43
		2.0–800.0	16			0.16	0.50
	Raw	20.1–90.0	21	13.0	1.00	0.39	0.63
		90.0–710.1	53	13.0	2.00	0.23	0.54
		20.1–710.1	74			0.28	0.57
Tl ⁺ -Xe	Smooth	20.0–120.0	6	14.0	1.00	0.35	0.37
		120.0–450.0	7	14.0	5.00	0.14	0.42
		20.0–450.0	13			0.24	0.40
	Raw	25.1–120.0	14	14.0	1.00	0.40	0.88
		120.0–352.4	28	14.0	5.00	-0.05	0.40
		25.1–352.4	42			0.10	0.60

^a Calculated products of the gas number density and the ion diffusion coefficient along the electrostatic field, n_0D_L , were obtained from the present potential. The smooth experimental data were taken from Ref. 18 and the raw experimental data were obtained from the gaseous ion transport database in Ref. 28.

Figure Captions

Figure 1

Calculated potential energy curves for the Tl^+-Rg complexes at the RCCSD(T) level of theory. Basis sets are of approximate aug-cc-pV5Z quality — see text for details.

Figure 2

Comparison between the calculated potential energy curves of the present work (solid lines) and the directly-determined potentials of ref. 14 (dotted lines).

Figure 3

Comparison between the experimental (solid line, points and error bars) and calculated (dotted line) mobilities for the Tl^+-Rg species ($Rg = He-Xe$). The differences between the two sets of values are barely discernible — see text for discussion. K_0 in $cm^2 V^{-1} s^{-1}$ and E/n_0 in Td.

Figure 4

Comparison between the experimental (solid line, points and error bars) and calculated (dotted line) $n_0 D_L$ values for the Tl^+-Rg species ($Rg = He-Xe$) — see text for discussion. $n_0 D_L$ in $10^{18} cm^{-1} s^{-1}$ and E/n_0 in Td.

FIGURE 1

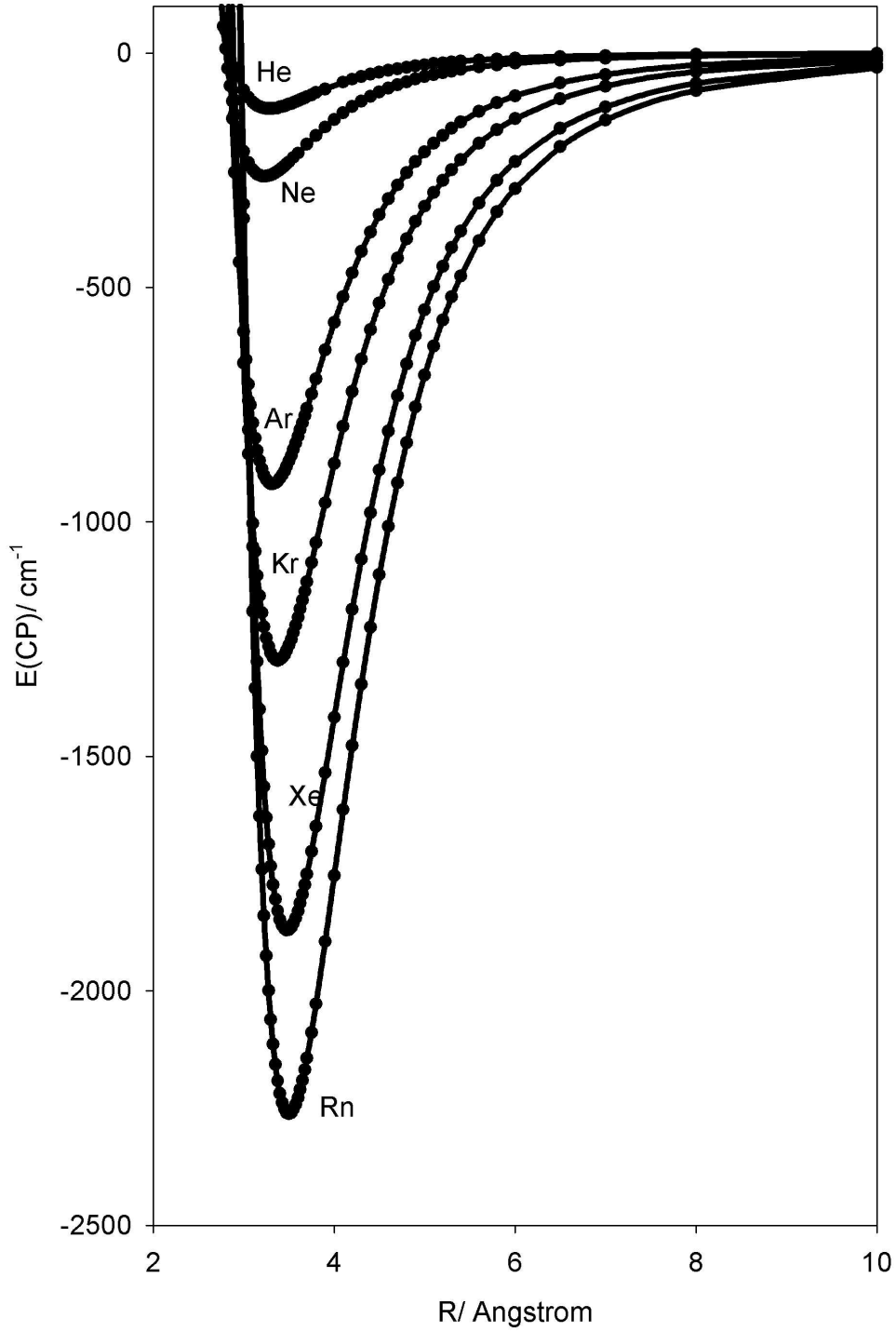
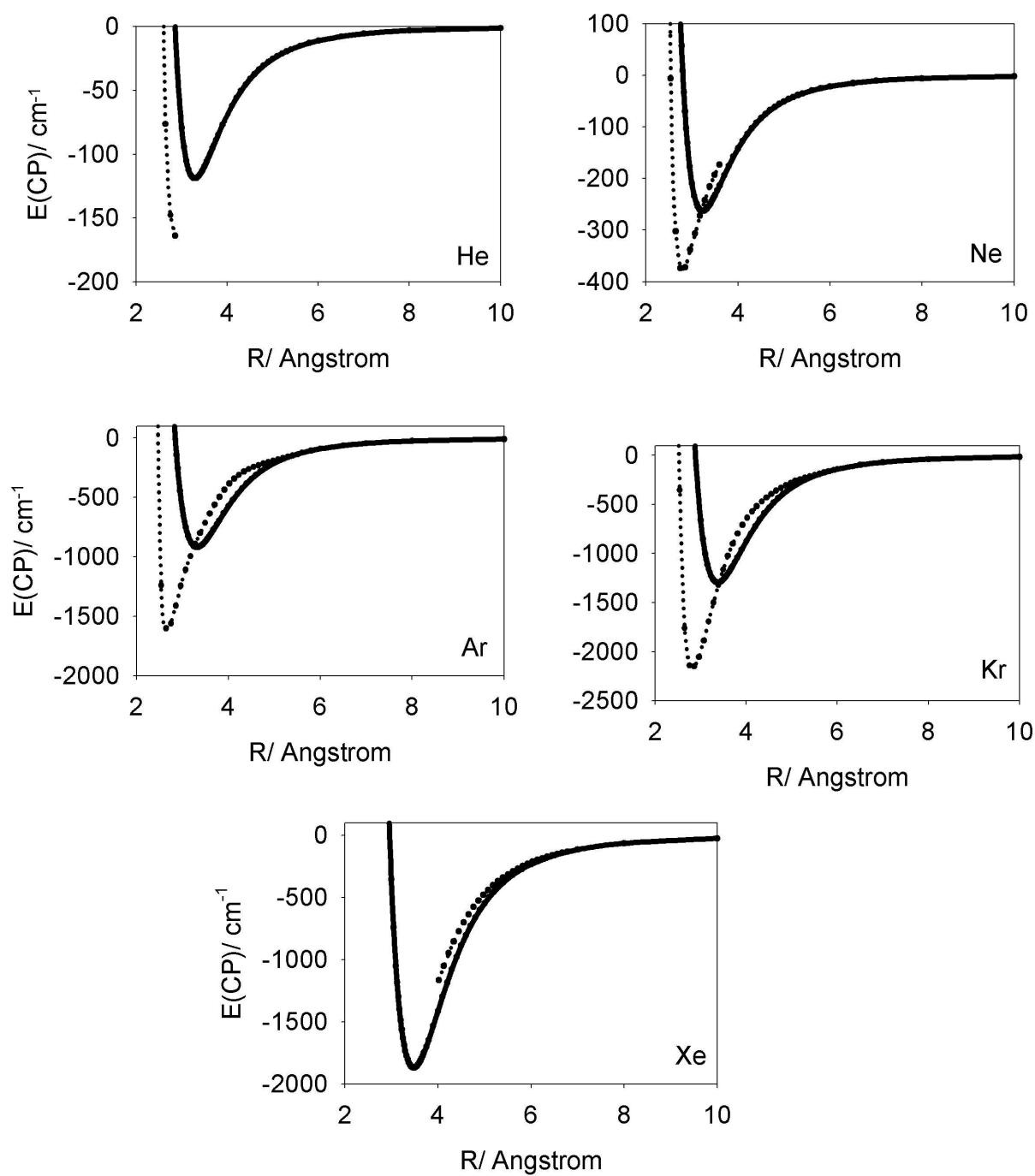


Figure 1, Gray et al.

Figure 2



Gray et al. Figure 2.

Figure 3

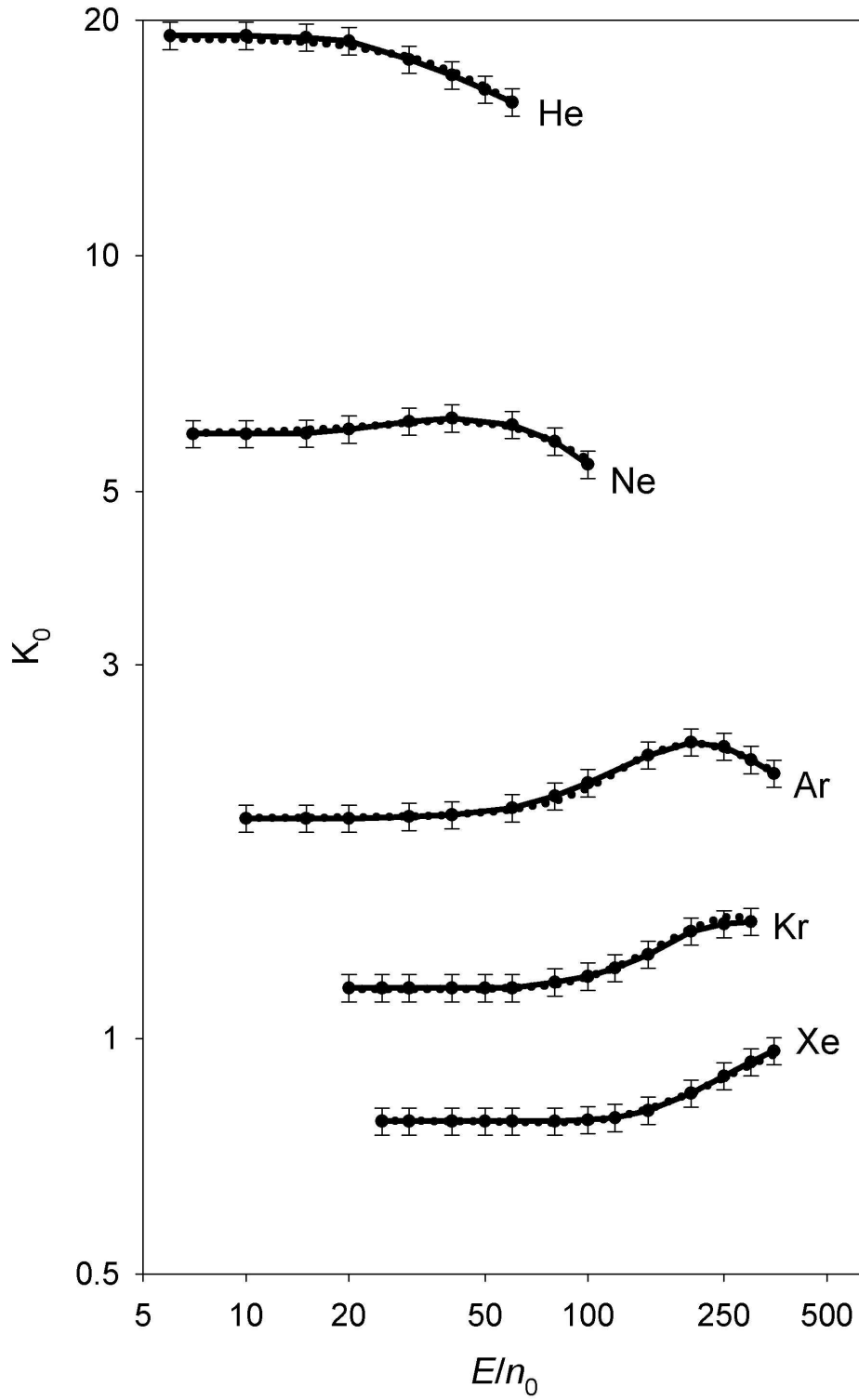


Figure 3 Gray et al.

Figure 4

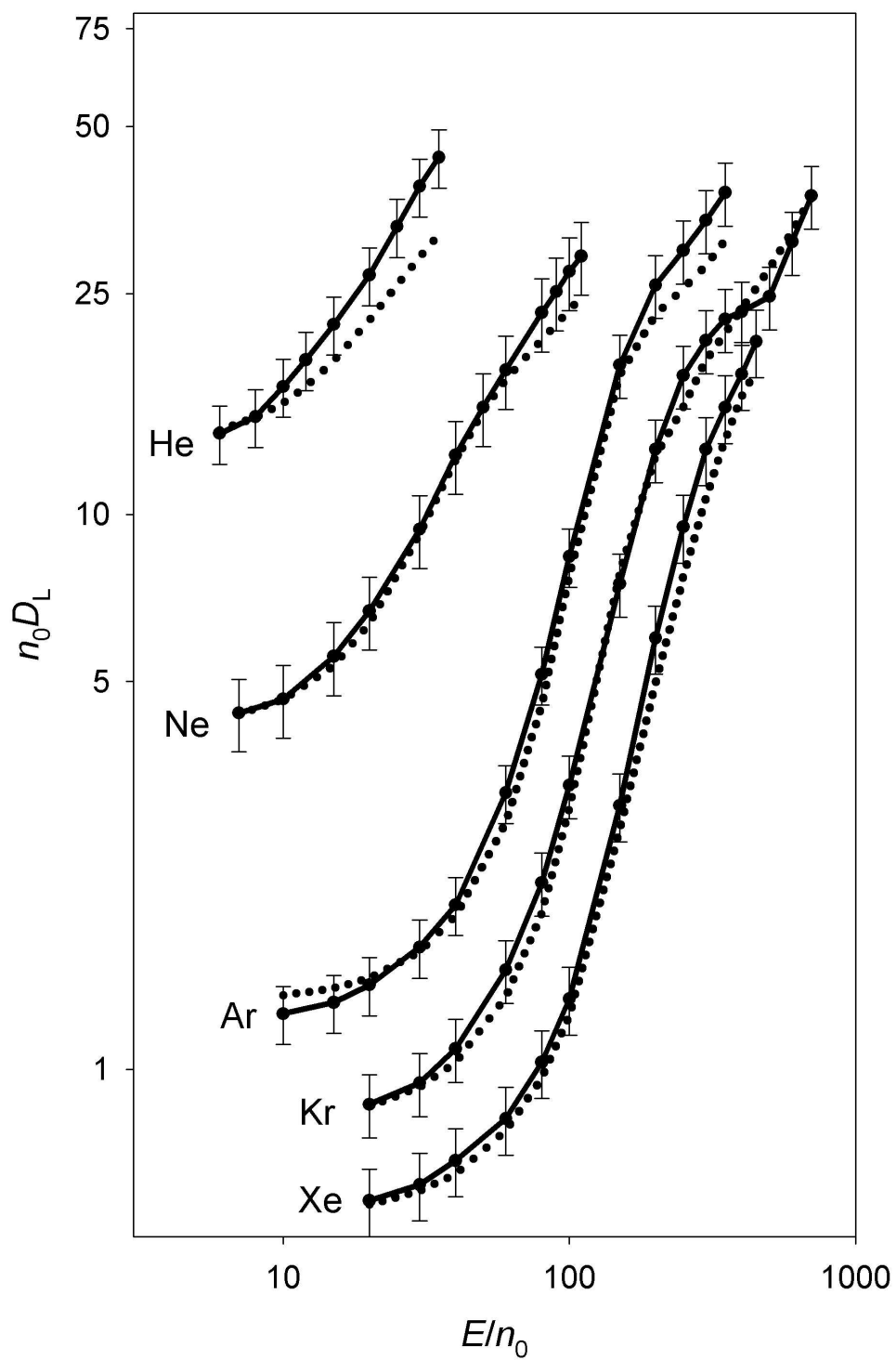


Figure 4 Gray et al.

References

- 1 J. Lozeille, E. Winata, L. A. Viehland, P. Soldán, E. P. F. Lee, and T. G. Wright, *Phys. Chem. Chem. Phys.*, **4**, 3601 (2002).
- 2 J. Lozeille, E. Winata, L. A. Viehland, P. Soldán, E. P. F. Lee and T. G. Wright, *J. Chem. Phys.*, **119**, 3729 (2003).
- 3 L. A. Viehland, J. Lozeille, P. Soldán, E. P. F. Lee, and T. G. Wright, *J. Chem. Phys.*, **121**, 341 (2004).
- 4 H. L. Hickling, L. A. Viehland, D. T. Shepherd, P. Soldán, E. P. F. Lee, and T. G. Wright, *Phys. Chem. Chem. Phys.*, **6**, 4233 (2004).
- 5 L. A. Viehland, R. Webb, E. P. F. Lee, and T. G. Wright, *J. Chem. Phys.*, **122**, 114302 (2005).
- 6 T. G. Wright and L. A. Viehland, *Chem. Phys. Lett.*, **420**, 24 (2006).
- 7 E. Qing, L. A. Viehland, E. P. F. Lee, and T. G. Wright, *J. Chem. Phys.* **124**, 044316 (2006).
- 8 D. M. Danailov, R. Brothers, L. A. Viehland, R. Johnsen, T. G. Wright, and E. P. F. Lee, *J. Chem. Phys.* (In press).
- 9 B. R. Gray, T. G. Wright, E. L. Wood, L. A. Viehland, *PCCP* (Submitted)
- 10 A. A. Buchachenko, J. Kłos, M. M. Szczyński, G. Chałasiński, B. R. Gray, T. G. Wright, E. L. Wood, L. A. Viehland, and E. Qing, *J. Chem. Phys.* **125** 064305 (2006).
- 11 M. S. Lee, A. S. Dickinson, and L. A. Viehland, *J. Phys. B.* **33**, 5121 (2000).
- 12 A. A. Buchachenko, R. V. Krems, M. M. Szczyński, Y.-D. Xiao, L. A. Viehland, and G. Chałasiński, *J. Chem. Phys.* **114**, 9919 (2001).
- 13 A. A. Buchachenko, T. V. Tscherebul, J. Kłos, M. M. Szczyński, G. Chałasiński, R. Webb, and L. A. Viehland, *J. Chem. Phys.* **122**, 194311 (2005).
- 14 C.C. Kirkpatrick and L. A. Viehland, *Chem. Phys.*, **120**, 235 (1988).
- 15 M. S. Byers, M. G. Thackston, R. D. Chelf, F. B. Holleman, J. R. Twist, G. W. Neeley, E. W. McDaniel, *J. Chem. Phys.* **78**, 2796 (1983).
- 16 M. G. Thackston, M. S. Byers, F. B. Holleman, R. D. Chelf, J. R. Twist, and E. W. McDaniel, *J. Chem. Phys.*, **78**, 4781 (1983).
- 17 R. D. Chelf, F. B. Holleman, M. G. Thackston, and E. W. McDaniel, *J. Chem. Phys.* **88**, 4551 (1988).
- 18 Mobility data for Tl^+ in He, Ne and Ar are taken from H. W. Ellis, M. G. Thackston, E. W. McDaniel and E. A. Mason, *Atomic and Nucl. Data Tables*, **31**, 113 (1984), where the data is referenced as F.B.Holleman, M.S. Byers, M.G. Thackston and E. W. McDaniel, to be published, but it does not seem to have been.

- 1
2
3 ¹⁹ L. A. Viehland and E. A. Mason, *Atomic and Nucl. Data Tables*, **60**, 37 (1995).
4
5 20 L. A. Viehland, *Chem. Phys.*, **78**, 279 (1983).
6
7 21 L. A. Viehland, *Chem. Phys.*, **85**, 291 (1984).
8
9 22 K. Raghavachari, G. W. Trucks, J. A. Pople, M. Head-Gordon, *Chem. Phys. Lett.*, **157**, 479
10 (1989); R. J. Bartlett, J. D. Watts, S. A. Kucharski, J. Noga, *ibid.*, **165**, 513 (1989).
11
12 23 MOLPRO is a package of ab initio programs written by H.-J. Werner, P.J. Knowles, with
13 contributions from J. Almlöf, R.D. Amos, A. Berning, M. J. O. Deegan, F. Eckert, S. T. Elbert,
14 C. Hampel, R. Lindh, W. Meyer, A. Nicklass, K. Peterson, R. Pitzer, A. J. Stone, P. R. Taylor,
15 M. E. Mura, P. Pulay, M. Schuetz, H. Stoll, T. Thorsteinsson, D. L. Cooper. The CCSD
16 treatment is described in: C. Hampel, K. Peterson, and H. J. Werner, *Chem. Phys. Lett.*, **190**, 1
17 (1992).
18
19 ²⁴ S. Johansson, G. Kalus, T. Brage, D. S. Leckrone, and G. M. Wahlgren, *Astrophys. J.* **462**, 943
20 (1996).
21
22 25 R. J. LeRoy, Level 7.2 – A computer program for solving the radial Schrödinger equation for
23 bound and quasibound levels, and calculating various values and matrix elements. University of
24 Waterloo Chemical Physics Research Program Report CP-555R, 2000.
25
26 26 L. A. Viehland, *Chem. Phys.*, **70**, 149 (1982).
27
28 27 L. A. Viehland, *Chem. Phys.*, **179**, 71 (1994).
29
30 28 L. A. Viehland, *Comp. Phys. Commun.*, **142**, 7 (2001).
31
32 29 E. A. Mason, E. W. McDaniel, *The Mobility and Diffusion of Ions in Gases* (Wiley, New York,
33 1988).
34
35 30 To access this database you must telnet to the computer named sassafrass.chatham.edu and
36 logon as gastrans. The required password will be provided upon request by email to
37 viehland@sassafrass.chatham.edu.
38
39 ³¹ T. H. Lovaas, H. R. Skullerud, O.-H. Kristensen, and D. Lihjell, *J. Phys. D* **20**, 1465 (1990).
40
41
42
43
44
45
46
47
48
49
50
51
52
53
54
55
56
57
58
59
60

Accurate Potential Energy Curves for Tl^+-Rg ($Rg = He-Rn$): Spectroscopy and Transport Coefficients

Benjamin R. Gray^a, Edmond P. F. Lee^b, Ahlam Yousef^c, Shraddha Shrestha^c,
Larry A. Viehland^{c 1}, and Timothy G. Wright^{a 2}

^a School of Chemistry, University of Nottingham, University Park, Nottingham, NG7
2RD, UK

^b School of Chemistry, University of Southampton, Highfield, Southampton, SO17
1BJ, UK and Department of Applied Biology and Chemical Technology, Hong Kong
Polytechnic University, Hung Hom, Hong Kong.

^c Division of Science, Chatham College, Pittsburgh, PA 15232, USA

¹ email: viehland@chatham.edu

² email: Tim.Wright@nottingham.ac.uk

Abstract

High-quality *ab initio* potential energy curves are presented for the Tl^+-Rg series ($Rg = He-Rn$). Calculations are performed at the CCSD(T) level of theory, employing aug-cc-pV5Z quality basis sets, with “small core” relativistic effective core potentials being used for Tl^+ and $Kr-Rn$. The curves are shown to be in excellent agreement with experimental mobility data for the systems Tl^+-Rg ($Rg = He-Xe$), and generally excellent agreement is also obtained with longitudinal diffusion data. An exception to the latter is Tl^+ in He, which is attributed to the experimental data not being obtained under steady state conditions. We also present spectroscopic information for the titular species, derived from our potential energy curves, and compare the results to previous potentials inferred from the ion transport data.

1. Introduction

This work continues our series of studies focused on the production of accurate atomic ion/rare gas atom interaction potentials. In this paper, as with the others in the series, we employ the potentials to obtain transport coefficients and spectroscopic data and compare these to experiment and theory where data are available. Other papers in this series concern: the 36 alkali metal/Rg systems;^{1, 2, 3, 4} O⁻ with He, Ne and Ar;⁵ S⁻ with He;⁶ Hg⁺ and Cd⁺ with all six Rg;⁷ O⁺ with He;⁸ F⁻ with all of the Rg;⁹ and Br⁻ with all of the Rg.¹⁰ One of us has also looked at ³He⁺ and ⁴He⁺ in their parent gases,¹¹ the Cl/Rg systems¹² and the I/Rg systems.¹³ In this paper we present six new interaction potentials between the group 13 ion, Tl⁺, and the rare gas atoms, Rg. The only previously-reported potentials appear to be the “directly determined” (DD) potentials¹⁴, i.e. those obtained from measurements^{15, 16, 17, 18, 19} of the gas-phase ion transport properties by inversion^{20, 21}. (Note that the smoothed versions of the original data^{15, 16, 17} used herein are reported in refs. 18, 19.)

The purpose of the present work is to determine *ab initio* potential energy curves for the Tl⁺-Rg systems over wide ranges of the ion-neutral separations. The potentials are employed to calculate spectroscopic constants and gaseous ion transport data. Where available, we compare these to the experimental and theoretical results mentioned above.

2. Computational Details

The potential energy curves were calculated point by point at the restricted coupled cluster level²², RCCSD(T), with single and double excitations and with the non-iterative correction to triple excitations, using the MOLPRO²³ suite of programs. The full counterpoise (CP) correction was employed at each point to correct for basis set superposition error (BSSE).

The calculations were run with augmented, all-electron quintuple- ζ basis sets (aug-cc-pV5Z) for He, Ne and Ar. We employed the “small-core” effective core potentials ECP10MDF, ECP28MDF and ECP60MDF for Kr, Xe and Rn, respectively; and an ECP60MDF one for Tl⁺. Tl has the electronic configuration, $\dots 5s^2 5p^6 5d^{10} 6s^2 6p^1$, and so the ground state is a ¹S state, with $\dots 6s^1 6p^1$ states lying $\sim 50,000$ cm⁻¹ higher in energy²⁴, and so not expected to interact with the ground state. Since there is no orbital angular momentum, then first-order spin-orbit coupling is not an issue here; in addition, the nearest $J = 0$ levels for Xe are over 76, 000 cm⁻¹ higher in energy, and even higher for the other lighter Rg atoms — even for Rn, it is unlikely there are complications arising from

1
2 **spin-orbit coupling.** There is, however, another complication present in running these calculations,
3 since the ordering of the orbitals changes. The Tl^+ $5s$ and $5p$ orbitals lie above the $1s2s2p$ orbitals
4 of Ar, and the $1s$ orbitals of Ne and He, and are correlated; but for the heavier rare gas atoms, the
5 Tl^+ $5s$ and $5p$ orbitals are lower than the valence electrons, and are uncorrelated. This places
6 different demands on the thallium basis set, and tight basis functions need to be added in to describe
7 better the correlation of the “outer core” $5s5p$ electrons. Thus, for the Tl^+ -Rg complexes involving
8 the lighter three rare gas atoms, the thallium basis set was as follows: the ECP60MDF ECP was
9 employed, with the standard aug-cc-pV5Z valence basis set, further augmented by tight functions:
10 three s functions ($\zeta = 10.0, 4.0$ and 1.6); three sets of p functions ($\zeta = 9.375, 3.75$ and 1.5); two d
11 functions ($\zeta = 3.125$ and 1.25); two f functions ($\zeta = 3.125$ and 1.25); a set of g functions ($\zeta = 1.35$);
12 and a set of h functions ($\zeta = 1.35$). For the calculations on Tl^+ -Rg complexes involving the three
13 heavier rare gas atoms, the additional s and p functions were omitted, as were the additional tightest
14 set of d and f functions. **As a check on the role of the $5s5p$ electrons of Tl^+ , we correlated these in**
15 **the case of Tl^+ -Ar, with an appropriate basis set, and found that R_e was essentially unchanged to**
16 **0.01 \AA , and D_e got larger by $< 12 \text{ cm}^{-1}$ when the $5s5p$ were correlated (amounting to an error of 1.3**
17 **%). We conclude that the non-correlation of the $5s5p$ electrons for the heavier species is unlikely to**
18 **have an important effect on the potential energy curves.** All standard exponents and contractions
19 were taken from the MOLPRO internal library. Once the counterpoise-corrected energy points
20 were obtained, they were used as input to LeRoy’s LEVEL²⁵ program, from which we were able to
21 calculate equilibrium nuclear separations, dissociation energies, and rovibrational energy levels.
22
23
24
25
26
27
28
29
30
31
32
33
34
35
36
37
38
39
40

41 Transport cross-sections and coefficients were calculated from the interaction potentials as a
42 function of ion-neutral collision energy using the programs QVALUES and GRAMCHAR.^{26,27,28}
43 The accuracies of the calculated mobilities and diffusion coefficients were 0.1% and 1.0%,
44 respectively, unless otherwise noted below.
45
46
47
48
49

50 **3. Results**

51 **A. Potential Curves**

52 The six potential curves are plotted in Figure 1 and the tabulated values (which extend both to
53 smaller and larger separation) are available from the authors upon request. The only other potential
54 energy curves available, the directly-determined ones, are shown in Figure 2, plotted against the
55 present curves. The differences between the present and the previous results will be discussed
56 briefly in this section, and in more detail after their abilities to reproduce the transport data are
57
58
59
60

discussed in the next section.

The parameters for each of our calculated potentials are given in Table I. They are: the separation, σ , at which the interaction energy is zero (on the repulsive wall); the equilibrium separation, R_e , at which the potential energy reaches its minimum value; and D_e , which is the depth of the potential well. The parameters show monotonic trends down the Rg group, with smooth decreases in σ and R_e and a reasonably smooth decrease in D_e —the non-periodicity of the directly-determined parameters¹⁴ was attributed to errors in the original transport data.

For $\text{Ti}^+\text{-He}$, the DD potential encompasses only a fragment of the repulsive wall and the start of the potential well. The DD wall is steeper and the zero energy separation is 0.25 \AA shorter than our potential, suggesting that the complete potential would probably be too strongly bound. For $\text{Ti}^+\text{-Ne}$, part of the repulsive wall is given by the DD potential as well as the potential well. Again, the wall is steeper and the zero energy value is 0.27 \AA shorter than our potential. Here we can also compare the equilibrium separation and the dissociation energy. The potential is too strongly bound, has too short an equilibrium separation, and has too deep a well, compared to the present potential. At around 3.2 \AA our potential and the DD potential cross (see Figure 2) and the latter appears to approach the dissociation limit above our curve.

For $\text{Ti}^+\text{-Ar}$, the behaviour is similar to Ne, with shorter zero energy and equilibrium distances, a deeper well, and a steeper repulsive wall. This time, however, the difference in dissociation energy is more pronounced, with the DD potential being almost twice as deep as the present potential, and with a bond length that is 0.7 \AA shorter. The trend continues for $\text{Ti}^+\text{-Kr}$ where a similarly large dissociation energy results from the DD potential, and a bond length that is 0.5 \AA too short.

For $\text{Ti}^+\text{-Xe}$, only a short section of the attractive region of the potential was previously generated to which to compare. The curves appear to be converging asymptotically to large R , but again, the trend suggests that the DD potential is too attractive. The results given here for $\text{Ti}^+\text{-Rn}$ appear to be the only ones available.

B. Spectroscopic Data

Our calculated spectroscopic parameters are given in Table II. The dissociation energy, D_0 , is given

1
2 as computed, while the vibrational constants, ω_e and $\omega_e x_e$, have been determined from the energies
3 of the three lowest vibrational levels with rotational quantum number $J = 0$. The rotational constant,
4 B_0 , and the centrifugal distortion constant, D_{J0} , have been obtained by fitting the energies of the
5 three lowest rotational energy levels for vibrational quantum number $v = 0$ to the standard energy
6 expression.
7
8
9

10 There are no experimental results with which to compare our values.
11
12
13

14 15 16 **C. Transport Data** 17

18
19
20 Gaseous ion mobility and diffusion coefficients serve as good tests of the accuracy of ion-neutral
21 interaction potentials over wide ranges of internuclear separation. This is because the data are often
22 available with fair to high accuracies over wide ranges of the gas temperature, T_0 , and of the ratio,
23 E/n_0 , of the electrostatic field strength to the gas number density in the drift-tube mass
24 spectrometers used for the experiments²⁹.
25
26
27

28
29
30 We have calculated diffusion coefficients and mobilities for thallium cations in the rare gases over
31 wide ranges of E/n_0 and at a variety of T_0 , and we have placed the results in the gaseous ion
32 transport database at Chatham College³⁰. In Fig. 3, we show the calculated mobilities at 300 K as
33 compared to the experimental values, with a corresponding comparison for diffusion coefficients
34 being presented in Figure 4. Statistical comparisons²¹ at 300 K are shown in Tables III and IV,
35 where N is the number of experimental values in the indicated range of E/n_0 , “Acc” is the estimated
36 accuracy given by experiment and “Prec” is the precision of our numerical calculations. The
37 statistical quantity δ is small if there is good agreement, with values above 1 or below -1 indicating
38 that the experimental values are significantly above or below the calculated values, respectively.
39 The statistical quantity χ is always positive and should not be much greater than $|\delta|$; larger values
40 indicate either that the data is scattered or that the comparison is significantly dependent upon E/n_0 .
41
42
43
44
45
46
47
48
49
50

51 For Tl^+ in He, the mobility values in Table III indicate that the potential is performing extremely
52 well, as the $|\delta|$ values are almost zero. However the $|\delta|$ value for the products, $n_0 D_L$, of the gas
53 number density and the ion diffusion coefficient parallel to the electrostatic field, given in Table IV,
54 are greater than 1, suggesting disagreement with experiment, as can be seen in Figure 4. It was
55 noted in the original experimental paper¹⁷ that there was disagreement between the $n_0 D_L$ values
56 predicted from the mobilities by generalized Einstein relations, despite these relations giving good
57 agreement for Tl^+ moving in Ne and Ar. It was concluded that the Tl^+ ions had not reached a steady
58
59
60

1
2 state in the drift tube filled with He, owing to the mass mismatch, and that this would lead to
3 disagreement with the calculated values, as was observed.
4
5

6
7 Transport properties calculated from the DD potential for $\text{Ti}^+\text{-He}$ are in approximately as good
8 agreement with the data as the present potential, even though the potentials themselves differ
9 significantly. We attribute this to the limited range of separations (4.20-5.40 bohr) that significantly
10 influence the transport coefficients over the small range of E/n_0 used in the experiments and the
11 rather smooth behaviour of the potential on this region of the repulsive wall. The DD procedure
12 requires knowledge of the position of the potential minimum, and without such knowledge it can
13 lead to many different potentials that describe the experimental data with about the same accuracy.
14 We conclude that the present potential is accurate based on the good agreement of the present
15 potential with the mobility data, and the recognized weakness of the experimental diffusion values.
16 In addition, the good agreement for the other systems (*vide infra*), using the same methodology,
17 also indicates that this potential is accurate.
18
19
20
21
22
23
24
25
26
27

28 For Ti^+ in Ne, we again observe extremely small values for $|\delta|$ values for the mobilities calculated
29 from the present potential, but this time we also obtain small values for the diffusion coefficients.
30 Thus both sets of data show excellent agreement through all regions of E/n_0 , and this may also be
31 seen in Figures 3 and 4. The good agreement with the diffusion data is in line with the good
32 agreement achieved in ref. 17 between the experimental and generalized Einstein relation values.
33 The values of $|\delta|$ are smaller than those reported in ref. 14 for the DD potential, although those
34 values are also less than 1. The experimental data for this system probes the repulsive wall and
35 only a small portion of the well, *i.e.* separations between 4.6 and 6.8 bohr, so the DD potential
36 directly inferred from these data are expected to have only fair accuracy, as shown in Fig. 2. We
37 conclude that our current potential is accurate.
38
39
40
41
42
43
44
45
46
47

48 For Ti^+ in Ar, our potential is in exceptionally good agreement with the mobility results over the
49 whole range of E/n_0 — see Table III and Figure 3. For the diffusion data, the results in Table IV are
50 broken into two groups, between $E/n_0 = 10\text{--}150$ Td ($1 \text{ Td} = 10^{-21} \text{ Vm}^2$) and $E/n_0 = 150\text{--}350$ Td.
51 The lower E/n_0 data shows good agreement between experiment and theory, however for the larger
52 E/n_0 values, the value of $|\delta|$ suggests a significant disagreement between the calculated experimental
53 and calculated data, although the $|\delta|$ value for the whole range is still good. Figure 4 shows this as
54 well, with the calculated diffusion data just coming outside the error bars at high E/n_0 . This is
55 likely a reflection of the known inaccuracies of the Georgia Tech diffusion data at high E/n_0 , owing
56 to an inadequate treatment of the raw arrival time spectra.³¹
57
58
59
60

1
2
3
4 Tl^+ in Kr continues the trend in this present series of potentials by producing excellent agreement
5 between experiment and theory over a very wide range of E/n_0 values, with good agreement seen
6 within each of the ranges as well. The indications are that the potential is consistent with the
7 experimental data over long-, mid- and short- R values — see Tables III and IV and Figures 3 and 4.
8
9 A very similar story holds for Tl^+ in Xe, and similar conclusions are drawn. There is no
10 experimental data with which to compare Tl^+ in Rn, but since the methodology is the same, we
11 assume that the potential is of a similar reliability.
12
13
14
15
16
17

18 4. Conclusions

19
20
21 We have calculated Tl^+ -Rg potentials over a wide range of separation, and have found that the
22 potentials are in excellent agreement overall with the available experimental data, well within the 3-
23 4% error bars on the mobility, and also generally within the 12–14% error bars on the diffusion
24 data. The level of theory employed is high, using the RCCSD(T) correlated method and large basis
25 sets, with small-core ECPs for the heavier atoms. We have noted that the $5s$ and $5p$ Tl^+ orbitals lie
26 above the valence orbitals of He, Ne and Ar, but below those of Kr, Xe and Rn. We chose to
27 correlate these for the lighter atoms, and included appropriate basis functions in the basis set to
28 account for this.
29
30
31
32
33
34
35
36

37
38 The only poor result is that observed for Tl^+ in He with respect to the value for the product, n_0D_L , of
39 the gas number density and the ion diffusion coefficient parallel to the electrostatic field, given in
40 Table IV. We have noted, however, that the original experimenters pointed out a disagreement
41 between the data and an approximate theoretical model, and concluded that their experimental data
42 was affected by the failure of the light helium to allow steady state conditions to be reached. In
43 light of this, and the overall good agreement for the other systems, we conclude that the present
44 calculated transport data is more reliable than the experimental data. The only other region of
45 disagreement was with the Ar high E/n_0 data for n_0D_L , and again, it is probably safe to assume that
46 the experimental data is unreliable.
47
48
49
50
51
52
53
54

55 In summary, apparently for the first time, we have presented tested potential energy curves for a
56 cation of a sixth-period element, interacting with each of the Rg atoms, and have shown that these
57 curves are in excellent agreement with the only available experimental data, and are thus accurate
58 descriptions of the Tl^+ -Rg interactions.
59
60

Acknowledgements

BRG is grateful for support via a studentship from the EPSRC. The authors are grateful to the EPSRC for the award of computer time at the Rutherford Appleton Laboratories under the auspices of the Computational Chemistry Working Party (CCWP), which enabled these calculations to be performed. The research of LAV was supported by the U. S. National Science Foundation under grant CHE-0414241.

For Peer Review Only

Table I. Parameters derived from the present $Tl^+ - Rg$ interaction potentials, compared to [the KV results](#) from ref. 14. (See text for details.)

Potential	Ref.	$\sigma / \text{\AA}^a$	$R_e / \text{\AA}$	D_e / cm^{-1}
$Tl^+ - He$	present	2.85	3.28	119.0
	KV	2.60	_b	_b
$Tl^+ - Ne$	present	2.81	3.23	263.1
	KV	2.54	2.85	372.0
$Tl^+ - Ar$	present	2.85	3.32	919.0
	KV	2.50	2.64	1600.6
$Tl^+ - Kr$	present	2.89	3.38	1295.3
	KV	2.54	2.86	2149.3
$Tl^+ - Xe$	present	2.96	3.48	1870.7
	KV	_b	_b	_b
$Tl^+ - Rn$	present	2.97	3.50	2262.0

^a σ is the distance at which the potential energy curve has a value of zero.

^b Curve derived in ref. 14, but portion was not wide enough to establish this parameter.

Table II. Calculated spectroscopic constants in cm^{-1} , with numbers in parentheses denoting the power of ten. (See text for details.)

System	D_0	ω_e	$\omega_e x_e$	B_0	D_{j0}
$\text{Tl}^+\text{-He}$	119.0	63.04	8.87	0.365	6.49(-05)
$\text{Tl}^+\text{-Ne}$	263.2	49.42	2.68	0.0865	1.22(-06)
$\text{Tl}^+\text{-Ar}$	919.1	62.46	1.20	0.0454	1.01(-07)
$\text{Tl}^+\text{-Kr}$	1295.3	53.44	0.62	0.0247	2.18(-08)
$\text{Tl}^+\text{-Xe}$	1870.7	52.84	0.41	0.0174	7.68(-08)
$\text{Tl}^+\text{-Rn}$	2262.0	49.33	0.29	0.0129	3.58(-09)

Table III. Statistical Comparison of Calculated and Experimental Mobility Data at 300 K.^a

System	Expt. Data	E/n_0 Range	N	Acc	Prec	δ	χ
Tl ⁺ -He	Smooth	6.0–60.0	8	4.00	0.02	0.05	0.25
	Raw	6.0–70.0	20	4.00	0.02	0.15	0.22
Tl ⁺ -Ne	Smooth	7.0–100.0	9	4.00	0.02	-0.07	0.18
	Raw	7.0–81.4	40	4.00	0.02	0.09	0.27
Tl ⁺ -Ar	Smooth	10.0–150.0	9	4.00	0.10	0.09	0.19
		150.0–350.0	4	4.00	0.10	0.03	0.08
		10.0–350.0	13			0.07	0.16
	Raw	10.0–150.0	45	4.00	0.10	0.15	0.47
		150.0–369.0	34	4.00	0.10	0.01	0.49
		10.0–369.0	79			0.09	0.48
Tl ⁺ -Kr	Smooth	20.0–80.0	7	3.00	0.02	0.12	0.13
		80.0–700.0	11	3.00	0.10	-0.33	0.40
		20.0–700.0	18			-0.16	0.33
	Raw	20.1–80.0	17	3.00	0.02	0.14	0.33
		80.0–710.1	57	3.00	0.10	-0.27	0.59
		20.1–710.1	74			-0.18	0.54
Tl ⁺ -Xe	Smooth	25.0–120.0	8	3.00	0.10	0.21	0.22
		120.0–350.0	5	3.00	0.50	-0.01	0.16
		25.0–350.0	13			0.13	0.20
	Raw	25.1–120.0	14	3.00	0.10	0.22	0.37
		120.0–352.4	28	3.00	0.50	0.12	0.58
		25.1–352.4	42			0.16	0.52

^a Calculated mobilities were obtained from the present potential. The smooth experimental data were taken from Ref. 18 and the raw experimental data were obtained from the gaseous ion transport database in Ref. 28. The statistical quantities δ and χ are described in the text, with a δ value close to zero representing good agreement between the theoretical and experimental data.

Table IV. Statistical Comparison of Calculated and Experimental Values of $n_0 D_L$ at 300 K.^a

System	Expt. Data	E/n_0 Range	N	Acc	Prec	δ	χ
Tl ⁺ -He	Smooth	6.0–35.0	9	12.0	1.00	1.31	1.66
	Raw	6.0–35.0	15	12.0	1.00	1.45	1.95
Tl ⁺ -Ne	Smooth	7.0–110.0	12	15.0	1.00	0.42	0.58
	Raw	7.0–81.4	71	15.0	1.00	0.29	0.55
Tl ⁺ -Ar	Smooth	7.0–150.0	9	12.0	1.00	0.22	0.59
		150.0–350.0	4	12.0	3.00	1.19	1.19
	Raw	7.0–350.0	13			0.52	0.83
		10.0–150.0	46	12.0	1.00	0.16	0.54
		150.0–250.0	28	12.0	2.00	0.72	0.98
		250.0–369.0	14	12.0	3.00	1.13	1.23
	10.0–369.0	88			0.49	0.84	
Tl ⁺ -Kr	Smooth	2.0–90.0	5	13.0	1.00	0.48	0.61
		90.0–800.0	11	13.0	2.00	0.02	0.43
		2.0–800.0	16			0.16	0.50
	Raw	20.1–90.0	21	13.0	1.00	0.39	0.63
		90.0–710.1	53	13.0	2.00	0.23	0.54
		20.1–710.1	74			0.28	0.57
Tl ⁺ -Xe	Smooth	20.0–120.0	6	14.0	1.00	0.35	0.37
		120.0–450.0	7	14.0	5.00	0.14	0.42
		20.0–450.0	13			0.24	0.40
	Raw	25.1–120.0	14	14.0	1.00	0.40	0.88
		120.0–352.4	28	14.0	5.00	-0.05	0.40
		25.1–352.4	42			0.10	0.60

^a Calculated products of the gas number density and the ion diffusion coefficient along the electrostatic field, $n_0 D_L$, were obtained from the present potential. The smooth experimental data were taken from Ref. 18 and the raw experimental data were obtained from the gaseous ion transport database in Ref. 28. The statistical quantities δ and χ are described in the text, with a δ value close to zero representing good agreement between the theoretical and experimental data.

1
2 **Figure Captions**
3

4
5 Figure 1
6

7 Calculated potential energy curves for the $\text{TI}^+\text{-Rg}$ complexes at the RCCSD(T) level of theory.
8 Basis sets are of approximate aug-cc-pV5Z quality — see text for details.
9

10
11
12 Figure 2
13

14 Comparison between the calculated potential energy curves of the present work (solid lines) and the
15 directly-determined potentials of ref. 14 (dotted lines).
16
17

18
19 Figure 3
20

21 Comparison between the experimental (solid line, points and error bars) and calculated (dotted line)
22 mobilities for the $\text{TI}^+\text{-Rg}$ species ($\text{Rg} = \text{He-Xe}$). The differences between the two sets of values are
23 barely discernible — see text for discussion. K_0 in $\text{cm}^2 \text{V}^{-1} \text{s}^{-1}$ and E/n_0 in Td.
24
25
26
27

28 Figure 4
29

30 Comparison between the experimental (solid line, points and error bars) and calculated (dotted line)
31 $n_0 D_L$ values for the $\text{TI}^+\text{-Rg}$ species ($\text{Rg} = \text{He-Xe}$) — see text for discussion. $n_0 D_L$ in $10^{18} \text{cm}^{-1} \text{s}^{-1}$
32 and E/n_0 in Td.
33
34
35
36
37
38
39
40
41
42
43
44
45
46
47
48
49
50
51
52
53
54
55
56
57
58
59
60

FIGURE 1

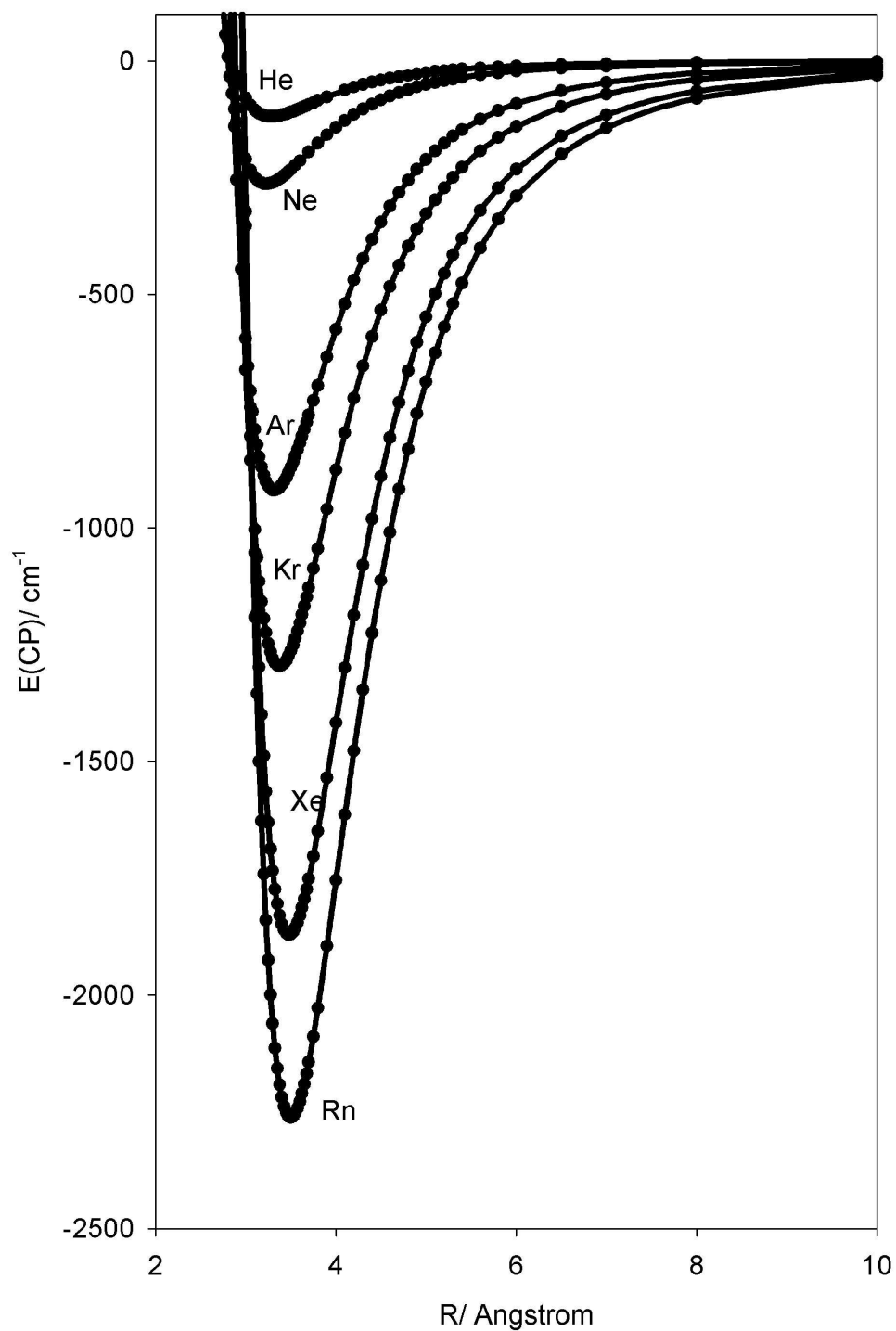
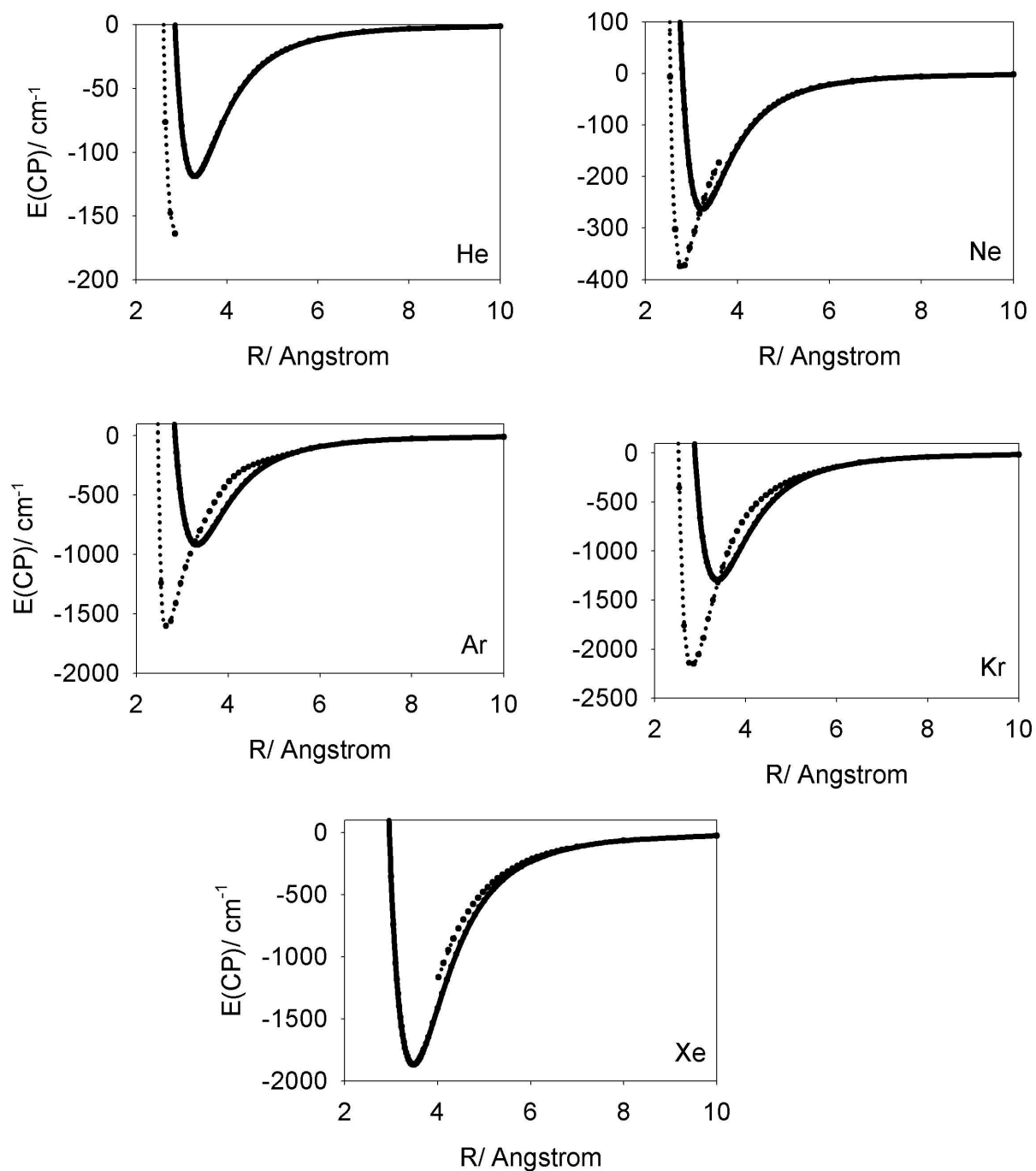


Figure 1, Gray et al.

Figure 2



Gray et al. Figure 2.

Figure 3

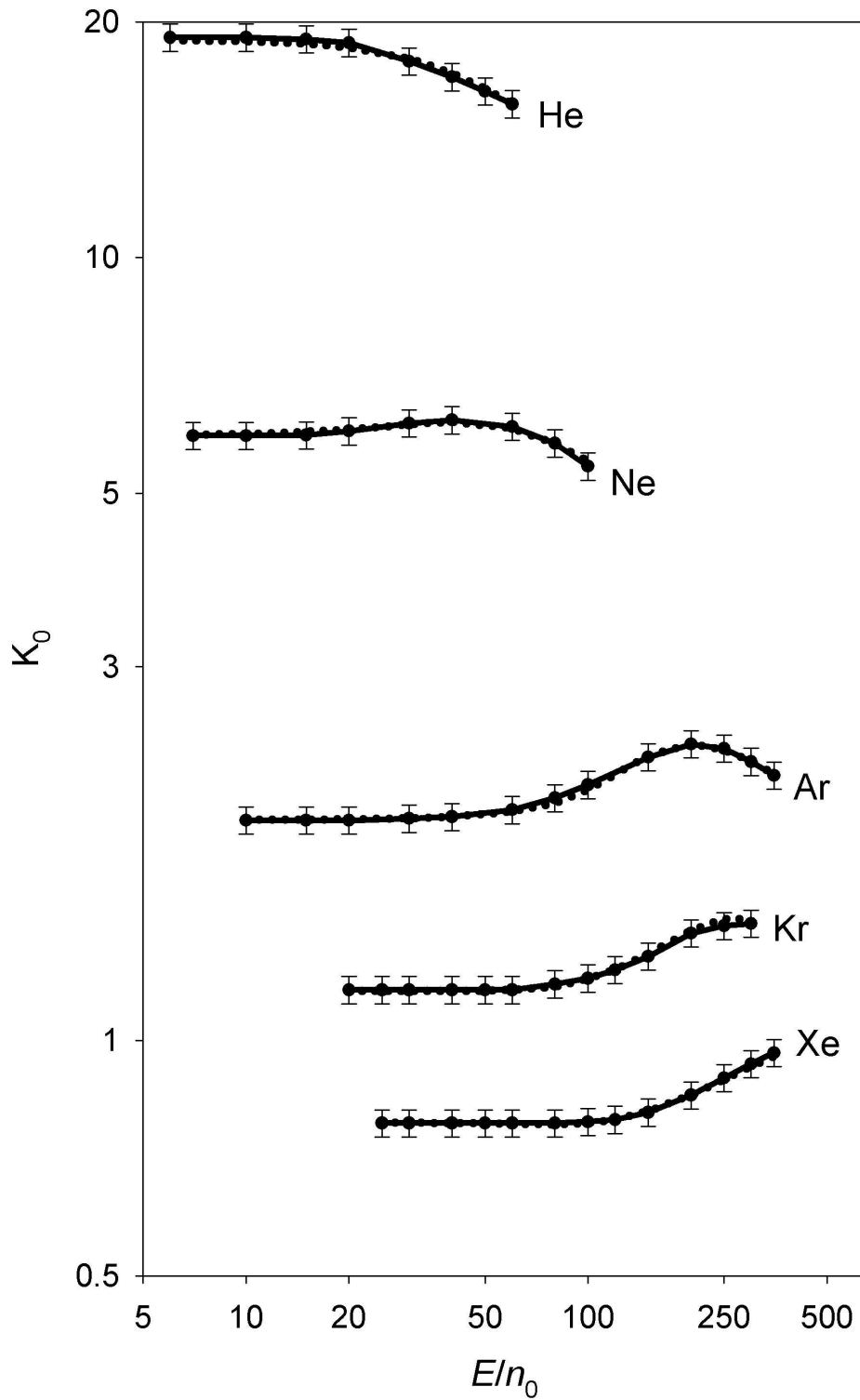


Figure 3 Gray et al.

Figure 4

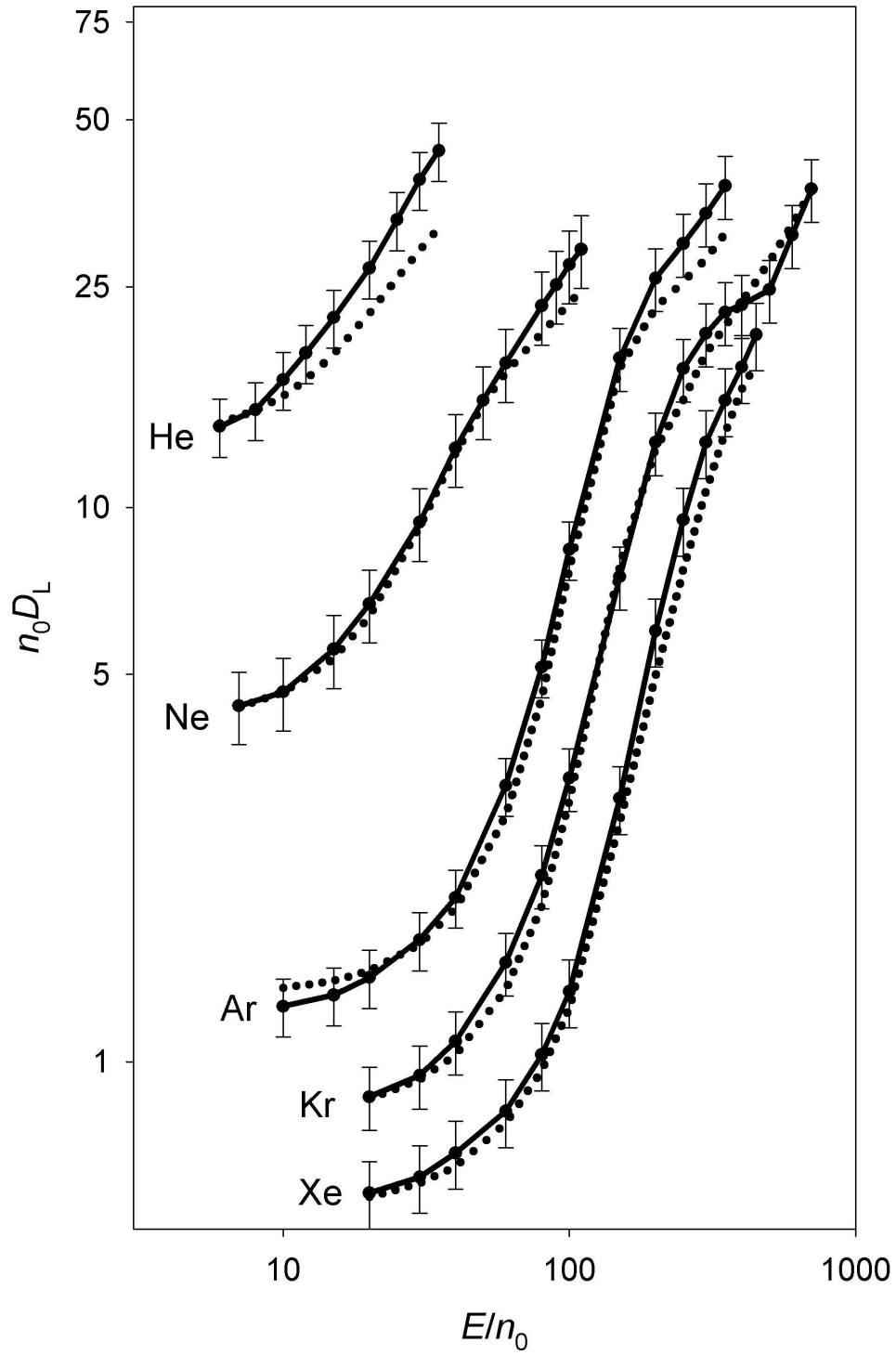


Figure 4 Gray et al.

References

- 1 J. Lozeille, E. Winata, L. A. Viehland, P. Soldán, E. P. F. Lee, and T. G. Wright, *Phys. Chem. Chem. Phys.*, **4**, 3601 (2002).
- 2 J. Lozeille, E. Winata, L. A. Viehland, P. Soldán, E. P. F. Lee and T. G. Wright, *J. Chem. Phys.*, **119**, 3729 (2003).
- 3 L. A. Viehland, J. Lozeille, P. Soldán, E. P. F. Lee, and T. G. Wright, *J. Chem. Phys.*, **121**, 341 (2004).
- 4 H. L. Hickling, L. A. Viehland, D. T. Shepherd, P. Soldán, E. P. F. Lee, and T. G. Wright, *Phys. Chem. Chem. Phys.*, **6**, 4233 (2004).
- 5 L. A. Viehland, R. Webb, E. P. F. Lee, and T. G. Wright, *J. Chem. Phys.*, **122**, 114302 (2005).
- 6 T. G. Wright and L. A. Viehland, *Chem. Phys. Lett.*, **420**, 24 (2006).
- 7 E. Qing, L. A. Viehland, E. P. F. Lee, and T. G. Wright, *J. Chem. Phys.* **124**, 044316 (2006).
- 8 D. M. Danailov, R. Brothers, L. A. Viehland, R. Johnsen, T. G. Wright, and E. P. F. Lee, *J. Chem. Phys.* (In press).
- 9 B. R. Gray, T. G. Wright, E. L. Wood, L. A. Viehland, *PCCP* (Submitted)
- 10 A. A. Buchachenko, J. Kłos, M. M. Szczyński, G. Chałasiński, B. R. Gray, T. G. Wright, E. L. Wood, L. A. Viehland, and E. Qing, *J. Chem. Phys.* **125** 064305 (2006).
- 11 M. S. Lee, A. S. Dickinson, and L. A. Viehland, *J. Phys. B.* **33**, 5121 (2000).
- 12 A. A. Buchachenko, R. V. Krems, M. M. Szczyński, Y.-D. Xiao, L. A. Viehland, and G. Chałasiński, *J. Chem. Phys.* **114**, 9919 (2001).
- 13 A. A. Buchachenko, T. V. Tscherebul, J. Kłos, M. M. Szczyński, G. Chałasiński, R. Webb, and L. A. Viehland, *J. Chem. Phys.* **122**, 194311 (2005).
- 14 C.C. Kirkpatrick and L. A. Viehland, *Chem. Phys.*, **120**, 235 (1988).
- 15 M. S. Byers, M. G. Thackston, R. D. Chelf, F. B. Holleman, J. R. Twist, G. W. Neeley, E. W. McDaniel, *J. Chem. Phys.* **78**, 2796 (1983).
- 16 M. G. Thackston, M. S. Byers, F. B. Holleman, R. D. Chelf, J. R. Twist, and E. W. McDaniel, *J. Chem. Phys.*, **78**, 4781 (1983).
- 17 R. D. Chelf, F. B. Holleman, M. G. Thackston, and E. W. McDaniel, *J. Chem. Phys.* **88**, 4551 (1988).
- 18 Mobility data for Tl^+ in He, Ne and Ar are taken from H. W. Ellis, M. G. Thackston, E. W. McDaniel and E. A. Mason, *Atomic and Nucl. Data Tables*, **31**, 113 (1984), where the data is referenced as F.B.Holleman, M.S. Byers, M.G. Thackston and E. W. McDaniel, to be published, but it does not seem to have been.

- 1
2
3 ¹⁹ L. A. Viehland and E. A. Mason, *Atomic and Nucl. Data Tables*, **60**, 37 (1995).
4
5 20 L. A. Viehland, *Chem. Phys.*, **78**, 279 (1983).
6
7 21 L. A. Viehland, *Chem. Phys.*, **85**, 291 (1984).
8
9 22 K. Raghavachari, G. W. Trucks, J. A. Pople, M. Head-Gordon, *Chem. Phys. Lett.*, **157**, 479
10 (1989); R. J. Bartlett, J. D. Watts, S. A. Kucharski, J. Noga, *ibid.*, **165**, 513 (1989).
11
12 23 MOLPRO is a package of ab initio programs written by H.-J. Werner, P.J. Knowles, with
13 contributions from J. Almlöf, R.D. Amos, A. Berning, M. J. O. Deegan, F. Eckert, S. T. Elbert,
14 C. Hampel, R. Lindh, W. Meyer, A. Nicklass, K. Peterson, R. Pitzer, A. J. Stone, P. R. Taylor,
15 M. E. Mura, P. Pulay, M. Schuetz, H. Stoll, T. Thorsteinsson, D. L. Cooper. The CCSD
16 treatment is described in: C. Hampel, K. Peterson, and H. J. Werner, *Chem. Phys. Lett.*, **190**, 1
17 (1992).
18
19 ²⁴ S. Johansson, G. Kalus, T. Brage, D. S. Leckrone, and G. M. Wahlgren, *Astrophys. J.* **462**, 943
20 (1996).
21
22 25 R. J. LeRoy, Level 7.2 – A computer program for solving the radial Schrödinger equation for
23 bound and quasibound levels, and calculating various values and matrix elements. University of
24 Waterloo Chemical Physics Research Program Report CP-555R, 2000.
25
26 26 L. A. Viehland, *Chem. Phys.*, **70**, 149 (1982).
27
28 27 L. A. Viehland, *Chem. Phys.*, **179**, 71 (1994).
29
30 28 L. A. Viehland, *Comp. Phys. Commun.*, **142**, 7 (2001).
31
32 29 E. A. Mason, E. W. McDaniel, *The Mobility and Diffusion of Ions in Gases* (Wiley, New York,
33 1988).
34
35 30 To access this database you must telnet to the computer named sassafrass.chatham.edu and
36 logon as gastrans. The required password will be provided upon request by email to
37 viehland@sassafrass.chatham.edu.
38
39 ³¹ T. H. Lovaas, H. R. Skullerud, O.-H. Kristensen, and D. Lihjell, *J. Phys. D* **20**, 1465 (1990).
40
41
42
43
44
45
46
47
48
49
50
51
52
53
54
55
56
57
58
59
60